

Structural Basis for the Inhibition of the Chromatin Repressor BAHD1 by the Bacterial Nucleomodulin LntA

Alice Lebreton,^{a,b,c} Viviana Job,^{d,e,f} Marie Ragon,^g Alban Le Monnier,^{g*} Andréa Dessen,^{d,e,f,h} Pascale Cossart,^{a,b,c} Hélène Bierne^{a,b,c*}

Institut Pasteur, Unité des Interactions Bactéries-Cellules, Paris, France^a; Institut National de la Santé et de la Recherche Médicale (INSERM), Paris, France^b; Institut National de la Recherche Agronomique (INRA), USC2020, Paris, France^c; Institut de Biologie Structurale (IBS), Université Grenoble Alpes, Grenoble, France^d; Commissariat à l'Énergie Atomique et aux Énergies Alternatives (CEA), Grenoble, France^e; Centre National de la Recherche Scientifique (CNRS), Grenoble, France^f; Institut Pasteur, French National Reference Center and WHO Collaborating Center for *Listeria*, Paris, France^g; Brazilian Laboratory for Biosciences (LNBio), CNPEM, Campinas, São Paulo, Brazil^h

* Present address: Alban Le Monnier, Université Paris 11, EA 4043, USC INRA, Chateau de Malabry, France, and Unité de Microbiologie Clinique et de Dosages des Anti-infectieux, Groupe Hospitalier Paris Saint-Joseph, Paris, France; Hélène Bierne, INRA, UMR1319 Micalis, F-78350 Jouy-en-Josas, France, and AgroParis Tech, UMR Micalis, F-78350 Jouy-en-Josas, France.

A.L. and V.J. contributed equally to this article.

ABSTRACT The nucleus has emerged as a key target for nucleomodulins, a family of effectors produced by bacterial pathogens to control host transcription or other nuclear processes. The virulence factor LntA from *Listeria monocytogenes* stimulates interferon responses during infection by inhibiting BAHD1, a nuclear protein involved in gene silencing by promoting heterochromatin formation. So far, whether the interaction between LntA and BAHD1 is direct and sufficient for inhibiting BAHD1 activity is unknown. Here, we functionally characterized the molecular interface between the two proteins *in vitro* and in transfected or infected human cells. Based on the known tridimensional structure of LntA, we identified a dilysine motif (K180/K181) in the elbow region of LntA and a central proline-rich region in BAHD1 as crucial for the direct LntA-BAHD1 interaction. To better understand the role played by the dilysine motif in the functionality of LntA, we solved the crystal structure of a K180D/K181D mutant to a 2.2-Å resolution. This mutant highlights a drastic redistribution of surface charges in the vicinity of a groove, which likely plays a role in nucleomodulin target recognition. Mutation of the strategic dilysine motif also abolished the recruitment of LntA to BAHD1-associated nuclear foci and impaired the LntA-mediated stimulation of interferon responses upon infection. Last, the strict conservation of residues K180 and K181 in LntA sequences from 188 *L. monocytogenes* strains of different serotypes and origins further supports their functional importance. Together, these results provide structural and functional details about the mechanism of inhibition of an epigenetic factor by a bacterial nucleomodulin.

IMPORTANCE Pathogens have evolved various strategies to deregulate the expression of host defense genes during infection, such as targeting nuclear proteins. LntA, a secreted virulence factor from the bacterium *Listeria monocytogenes*, stimulates innate immune responses by inhibiting a chromatin-associated repressor, BAHD1. This study reveals the structural features of LntA required for BAHD1 inhibition. LntA interacts directly with a central domain of BAHD1 via a surface patch of conserved positive charges, located nearby a groove on the elbow region of LntA. By demonstrating that this patch is required for LntA function, we provide a better understanding of the molecular mechanism allowing a bacterial pathogen to control host chromatin compaction and gene expression.

Received 12 September 2013 Accepted 10 December 2013 Published 21 January 2014

Citation Lebreton A, Job V, Ragon M, Le Monnier A, Dessen A, Cossart P, Bierne H. 2014. Structural basis for the inhibition of the chromatin repressor BAHD1 by the bacterial nucleomodulin LntA. *mBio* 5(1):e00775-13. doi:10.1128/mBio.00775-13.

Editor Olaf Schneewind, The University of Chicago

Copyright © 2014 Lebreton et al. This is an open-access article distributed under the terms of the [Creative Commons Attribution-NonCommercial-ShareAlike 3.0 Unported license](https://creativecommons.org/licenses/by-nc-sa/4.0/), which permits unrestricted noncommercial use, distribution, and reproduction in any medium, provided the original author and source are credited.

Address correspondence to Hélène Bierne, helene.bierne@jouy.inra.fr, or Andréa Dessen, andrea.dessen@ibs.fr.

The food-borne pathogen *Listeria monocytogenes* is the etiological agent of listeriosis, a disease with serious outcomes in the elderly, immunocompromised individuals, and fetuses or newborns (1). The virulence potential of *Listeria* resides mainly in its ability to cross the host intestinal, fetoplacental, and blood-brain barriers, allowing its dissemination throughout the organism, unless its replication is controlled by an efficient innate host immune response (2, 3). *L. monocytogenes* can enter and multiply in the cytosol of most human cell types and spread to neighboring cells, thereby avoiding host humoral immune defenses. Bacterial clearance is thus mostly driven by cell-mediated immunity.

A successful infectious process relies on an arsenal of virulence factors that target diverse cellular components and subsequently hijack various host cell functions (4–6). Not surprisingly, a set of listerial factors is able to reprogram host transcriptional responses in order to deregulate defense genes. For instance, internalins InlB and InlC modulate cytoplasmic signaling pathways leading to the activation, sequestration, or degradation of transcription factors (7, 8). Other factors, such as listeriolysin O (LLO) and LntA, target host transcription at the chromatin level (9, 10). While the pore-forming toxin LLO promotes deacetylation of histone H4 and dephosphorylation of histone H3 by an indirect mechanism in-

volving K^+ efflux (9, 11), LntA acts directly in the nucleus to manipulate a chromatin-regulatory protein (10, 12). Studying how these bacterial molecules interfere with the chromatin-based regulation process could provide evidence as to whether and how bacteria might alter epigenetic marks and machineries (13).

The protein LntA from *L. monocytogenes* localizes to the nuclei of infected cells, like other members of the emerging class of bacterial effectors termed “nucleomodulins” (14). Nucleomodulins can affect host gene expression by mimicking eukaryotic transcription factors or chromatin modifiers, or by targeting chromatin regulatory factors. However, how such proteins interact with components of chromatin-associated complexes at the molecular level remains to be characterized. Listerial LntA illustrates this property and is thus an interesting tool for dissecting host gene regulation by chromatin remodeling.

The search for LntA host partners led us to characterize a novel chromatin repressor, BAHD1 (15). We have shown that human BAHD1 stimulates chromatin compaction and heterochromatin formation, resulting in gene silencing. BAHD1 acts in partnership with other chromatin factors known to play important roles in chromatin-based repression, such as HP1, MBD1, SETDB1, histone deacetylases (HDACs), and KAP1 (10, 15). The set of genes repressed by the BAHD1-associated complex likely depends on the cell type, as well as on the signal to which cells are submitted. In particular, BAHD1 represses interferon-stimulated genes (ISGs) in epithelial cells infected with *L. monocytogenes* (10). When *L. monocytogenes* expresses *LntA*, the secreted factor LntA enters the nucleus and alleviates BAHD1 binding to ISG promoters, thereby upregulating their expression. By preventing recruitment of BAHD1 and HDAC1/2 at ISG promoters, LntA is thought to trigger chromatin unwinding. We have proposed that the LntA-BAHD1 interplay spatiotemporally modulates the interferon (IFN) response to control bacterial colonization of the host (12). However, how LntA impairs the function of BAHD1 remains to be deciphered; in particular, whether a direct interaction between LntA and BAHD1 is required for such inhibition is unknown.

LntA is a small basic protein with no sequence homology to any known protein. We have previously solved the structure of LntA and shown that it folds into a compact, elongated five-helix bundle (Protein Data Bank [PDB] accession number 2XL4; see also reference 10). In this study, we unravel the determinants involved in the LntA-BAHD1 interaction using crystallography, *in vitro* interaction assays, immunofluorescence, and functional assays after *Listeria* infections of human cells. Our results provide evidence that a direct interaction between the elbow domain of LntA and a proline-rich region in BAHD1 is required for stimulating innate immune gene expression, thus adding a molecular basis for the LntA-mediated inhibition of BAHD1.

RESULTS

LntA directly interacts with BAHD1 *in vitro*. BAHD1 is an 84.5-kDa basic protein that harbors a C-terminal bromo-adjacent homology (BAH) domain (Fig. 1A and see Fig. S1A in the supplemental material), which is found in various chromatin-associated proteins (16). A bipartite nuclear localization signal (NLS) is predicted within an arginine-rich region. The N-terminal region of the protein is rich in proline residues, with the highest density (24.4%) being found in a central proline-rich region (cPRR) extending from residues 239 to 361. The shortest interaction domain

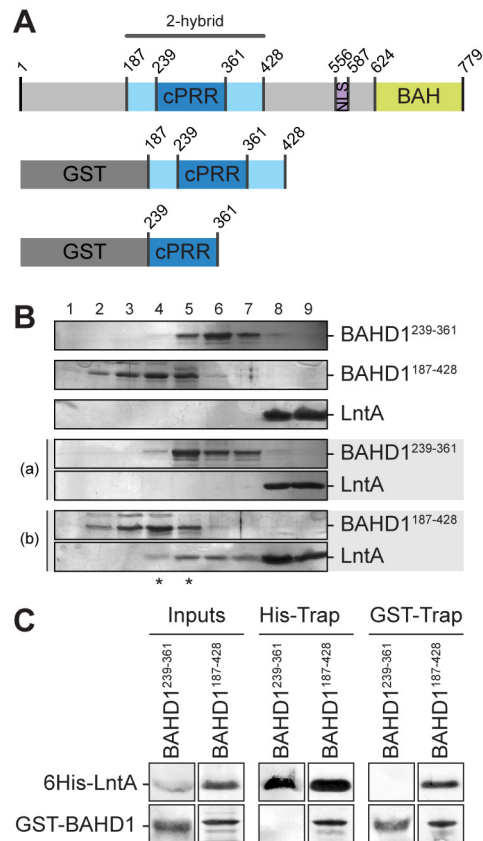


FIG 1 LntA interacts *in vitro* with BAHD1¹⁸⁷⁻⁴²⁸. (A) Primary structure of BAHD1. GST-BAHD1¹⁸⁷⁻⁴²⁸ and GST-BAHD1²³⁹⁻³⁶¹ fusions were tested for interaction with LntA. cPRR, central proline-rich region; NLS, nuclear localization signal; BAH, bromo-adjacent homology domain. (B) Gel filtration experiment. Purified LntA, GST-BAHD1¹⁸⁷⁻⁴²⁸, or GST-BAHD1²³⁹⁻³⁶¹, incubated alone or coincubated for 3 h at 4°C, were injected on a Superdex 200 column. Elution fractions (lanes 1 to 9) were analyzed by SDS-PAGE followed by Coomassie blue staining. Elution fractions of single proteins are shown in the first three lines; those of coincubated proteins are highlighted in the gels labeled a and b. *, coelution of LntA and GST-BAHD1¹⁸⁷⁻⁴²⁸. (C) 6His-LntA was coexpressed in *E. coli* with GST-BAHD1¹⁸⁷⁻⁴²⁸ or GST-BAHD1²³⁹⁻³⁶¹. Input and eluted fractions from pulldown assays on His-Trap or GST-Trap columns were analyzed by immunoblotting against the GST or the 6His tag.

with LntA identified by the yeast two-hybrid assay extends from residues 187 to 428 (10), thus encompassing the cPRR.

The secreted, mature form of LntA is a 19.7-kDa basic protein where K and R residues represent 18.6% of the sequence (Fig. S1B). Acidic residues also span 17.5% of the sequence and thus provide an important contribution to the global charge and hydrophilic properties of the protein. A putative bipartite NLS in LntA may participate in its nuclear localization.

In order to characterize the interaction between LntA and BAHD1 *in vitro*, we expressed and purified the individual proteins in *Escherichia coli* BL21 (DE3). LntA was produced with a glutathione *S*-transferase (GST) cleavable tag and was purified to homogeneity. In contrast, full-length BAHD1 could not be produced in *E. coli*; we thus tested two different GST-tagged BAHD1 constructs: one coding for the complete two-hybrid interaction domain, from residues 187 to 428 (BAHD1¹⁸⁷⁻⁴²⁸), and a second one harboring only the cPRR (BAHD1²³⁹⁻³⁶¹) (Fig. 1A). These two GST fusion proteins were well expressed and purified but showed

a high level of degradation upon SDS-PAGE (data not shown). We assessed a direct interaction between LntA and BAHD1 by a gel filtration assay (Fig. 1B). When tested alone, GST-BAHD1^{239–361} (39 kDa) eluted in fractions 5 to 7, while GST-BAHD1^{187–428} (52 kDa) eluted in fractions 2 to 5. LntA eluted in fractions 8 to 9, as expected for a protein of 20 kDa. When purified LntA and GST-BAHD1 fusions were coincubated prior to injection, LntA coeluted only with GST-BAHD1^{187–428} in fractions 4 to 5. We conclude that BAHD1^{187–428}, but not BAHD1^{239–361}, can form a stable complex with LntA *in vitro*.

These results were confirmed by different pull-down experiments where the 6His-LntA and GST-BAHD1 constructs were expressed separately (not shown) or coexpressed (Fig. 1C) in *E. coli*. In 6His pull-down assays as well as in GST pull-down assays, only BAHD1^{187–428} coeluted with 6His-LntA. The coexpression and GST pull-down assays subsequently allowed us to devise a rapid method to test protein complex formation and was useful for screening mutants, as shown below.

LntA can therefore interact *in vitro* with the central region (amino acids 187–428 of BAHD1). This and our previous results (10) thus support a direct interaction between LntA and BAHD1 without any additional factor, as it was observed in three independent systems: in *E. coli* using recombinant proteins, in *Saccharomyces cerevisiae* by two-hybrid screening, and in human cells by pull-down and microscopy assays.

A basic patch on the surface of LntA is involved in the interaction with BAHD1^{187–428}. LntA folds into a compact structure composed of five helices (PDB accession number 2XL4) (Fig. 2A and S1C): three long antiparallel helices (H1 to H3), which we refer to as the trunk of the protein, and two smaller ones (H4 and H5), which form a protruding elbow. The trunk is stabilized by a ladder of hydrophobic residues that also includes residues from H5, attesting to the compact nature of the structure. The surface of LntA presents distinct major charged patches (Fig. 2B) that may be involved in the interaction with protein partners, such as BAHD1. Patch 1, located at the “bottom” of LntA, is highly acidic and is formed mainly by residues E91, D98, and D102. Patch 2, on LntA’s side, is a basic region involving residues K125, K138, and K142 from H2 and H3. Patch 3, located on the opposite side of LntA, is a second highly basic region, shaped by residues K180, K181, R183, and K186 in H5. The potential importance of these residues for mediating functional interactions is further supported by their very robust conservation among *L. monocytogenes* strains (Fig. S5, commented upon below). Other charged residues also decorate the surface of LntA but are less likely to mediate interactions with BAHD1, either because they are less conserved or because they are involved in intramolecular interactions.

We investigated whether these regions could participate in BAHD1 recognition by designing site-specific mutants of each patch and comparing their abilities to bind BAHD1^{187–428} in GST pull-down assays (Fig. 3A). Distinct 6His-tagged LntA mutants had mutations aimed at reversing charges in each patch: E91R and E91R/D98K/D102K, targeting patch 1; K138D/K142D and K125D/K138D/K142D, targeting patch 2; and K180D/K181D and K180D/K181D/R183E/K186D, targeting patch 3. Only the patch 3 mutants abolished the interaction with GST-BAHD1^{187–428}. These results suggested that either (i) patch 3 is implicated in the interaction with BAHD1 or (ii) patch 3 mutants are folded incorrectly and thus can no longer bind BAHD1.

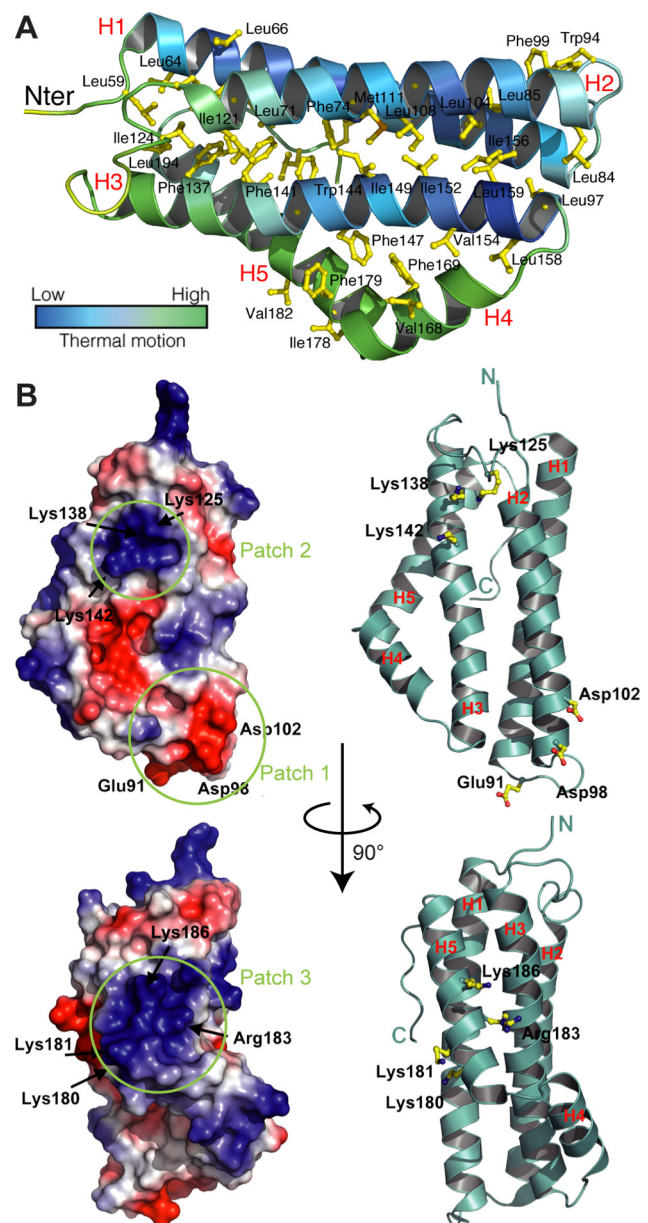


FIG 2 The surface of LntA displays two major basic patches and one acidic patch. (A) LntA folds into a compact helical structure that is stabilized by a ladder of hydrophobic residues, indicated as yellow sticks. The thermal-motion color scale (B-factor values) indicates that the body formed by H1, H2, and H3 is the less mobile region and that the H4-H5 elbow displays more flexibility. Nter, N terminus. (B) The three main charged patches targeted by mutagenesis are shown (green circles) on the electrostatic surface views of LntA. Basic regions are in blue and acidic regions in red. Patch-forming residues are shown as sticks.

LntA^{K180D/K181D} displays a local redistribution of surface charges without major structural changes in the LntA fold. In order to discriminate between these two possibilities, we characterized the properties of LntA with the K180D and K181D mutations (LntA^{K180D/K181D}), the minimal mutant allowing a loss of interaction with BAHD1^{187–428}, through biophysical assays, including thermal stability tests, gel filtration, and one-dimensional nuclear magnetic resonance (1D-NMR) (Fig. S2). LntA^{K180D/K181D}

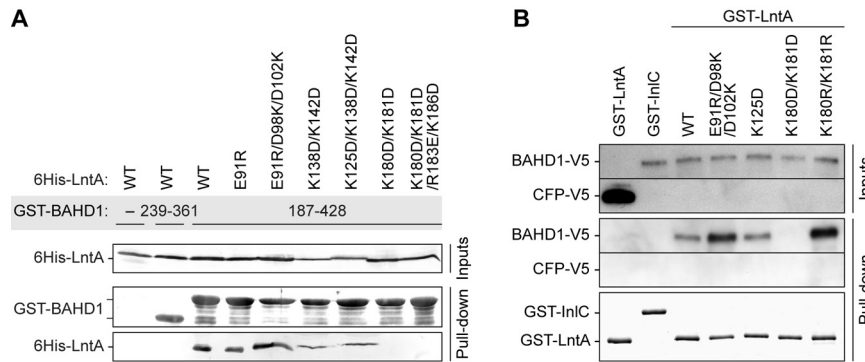


FIG 3 Positive charges in patch 3 of LntA are critical for interaction with BAHD1. (A) 6His-tagged LntA^{WT} and LntA mutants coexpressed with GST-BAHD1^{187–428} in *E. coli* were used for GST pull-down assays. 6His-LntA^{WT} alone and 6His-LntA^{WT} coexpressed with GST-BAHD1^{239–361} were used as negative controls. Proteins were detected by immunoblotting against the tags. (B) GST-tagged LntA^{WT}, LntA mutants, or InIC bound to glutathione-Sepharose was incubated with chromatin extracts containing full-length BAHD1-V5 or CFP-V5 as a negative control. V5-tagged fusions were detected by immunoblotting. GST-fused baits were detected by colloidal Coomassie blue staining.

was folded and stable; hence, the observed lack of interaction with GST-BAHD1^{187–428} did not proceed from improper folding. We conclude that the positive charges contributed by the K180/K181 dilysine motif in surface patch 3 are required for the interaction with BAHD1^{187–428} *in vitro*.

We then investigated in atomic detail how the mutation of these two critical lysines in helix 5 affected the structure of LntA and the interaction surface. We crystallized and solved the three-dimensional structure of LntA^{K180D/K181D} to a 2.22-Å resolution (Fig. 4). The structure was solved by performing a MR-SAD (molecular replacement combined with single-wavelength anomalous dispersion) experiment with data for the selenomethionine edge collected at the BM14 beamline of the European Synchrotron Radiation Facility (ESRF) and by using the model of wild-type LntA (LntA^{WT}) (PDB accession number 2XL4) for the MR phasing protocol. Data collection and refinement statistics can be found in Table S1. The overall fold of LntA^{K180D/K181D} is very similar to that of the wild-type protein (Fig. 4A, ribbon overlay), in agreement with a measured root mean square deviation of only 0.47 Å for 139 α carbons when the two structures were compared. The main difference involves the local modification of charges in the region of the double mutation, with disappearance of basic patch 3. This considerably increases the acidity at the closing end of an elongated groove within the LntA surface (Fig. 4B, arrows). Modifications of the electrostatic environment of this region are likely responsible for the loss of interaction between the two partners.

The K180/K181 dilysine motif is required for the interaction of LntA with full-length BAHD1. We next addressed whether LntA^{K180D/K181D} also lost its capacity to bind BAHD1 produced in human cells (Fig. 3B), reasoning that the full-length BAHD1 protein and/or its posttranslational modifications might stabilize the interaction with LntA. A BAHD1-V5 fusion was expressed in human embryonic kidney-derived cells (293FT). Solubilized chromatin extracts from these cells were incubated with wild-type or mutant forms of GST-LntA bound to a glutathione-Sepharose resin. In addition to the K180D/K181D mutant, GST-tagged LntA mutants in patches 1 and 2 were also assessed: the E91R/D98K/D102K mutant in patch 1, which was the most mutated variant that still maintained an interaction with BAHD1^{187–428} (Fig. 3A), and a K125D mutant in patch 2, because K138D/K142D mutants displayed a significant expression defect likely indicative of abnor-

mal folding (Fig. 3A). The GST-tagged secreted listerial factor InIC or the V5-tagged cyan fluorescent protein (CFP) was used as a negative control. GST-LntA was able to interact efficiently with BAHD1-V5, in agreement with our previous findings (10), as well as the mutants in patches 1 and 2, confirming that these exposed charges do not play important roles in the formation of the LntA-BAHD1 complex. In contrast, patch 3 mutant LntA^{K180D/K181D} showed no binding with full-length BAHD1-V5, as described above for BAHD1^{187–428}. Note that the E91R/D98K/D102K mutant in patch 1 displays an even stronger interaction with BAHD1 than LntA^{WT} (Fig. 3A and B). Possibly, the increase in basic charges brought about by this mutant might reinforce the attraction exerted by basic patch 3.

Lysine residues are often the targets of conjugation on their free ε-amino group, in bacteria as well as in eukaryotes (17, 18). To determine whether the loss of binding observed with the K180D/K181D mutant was due to the charge modification of its surface or to a loss of conjugation, we designed a K180R/K181R mutant which would keep the positive charge of the patch while thwarting any potential conjugation at that site. This mutant was still able to pull down BAHD1-V5 (Fig. 3B) with even stronger efficiency than GST-LntA^{WT}, thus ruling out the possibility that the binding defect observed with the K180D/K181D mutant is due to the absence of a posttranslational modification of lysines.

The dilysine motif in LntA and the central proline-rich region in BAHD1 are required for colocalization of the two proteins in human cells. We have previously shown that, when overexpressed in human cells, BAHD1 stimulates the formation of heterochromatic nuclear foci. In addition, it is targeted to the inactive X chromosome (Xi) in female cells (15). In particular, in the hypotriploid female cell line 293FT, which contains three copies of the X chromosome, BAHD1-yellow fluorescent protein (YFP) colocalizes with the two inactive Xi (15). Transfection of LntA^{WT}-V5 alone into 293FT cells resulted in uniform nuclear labeling with no clear local enrichment (Fig. S3A), as previously observed in C3SV40 fibroblasts (10). When LntA^{WT}-V5 was coexpressed with BAHD1-YFP in 293FT, LntA^{WT}-V5 was enriched in BAHD1-YFP-induced heterochromatin foci (Fig. 5 and Fig. S3B), as in fibroblasts (10); in addition, the LntA^{WT}-V5 signal was also very dense in the two large Xi areas marked by BAHD1-YFP. In striking contrast, the LntA^{K180D/K181D}-V5 mutant was

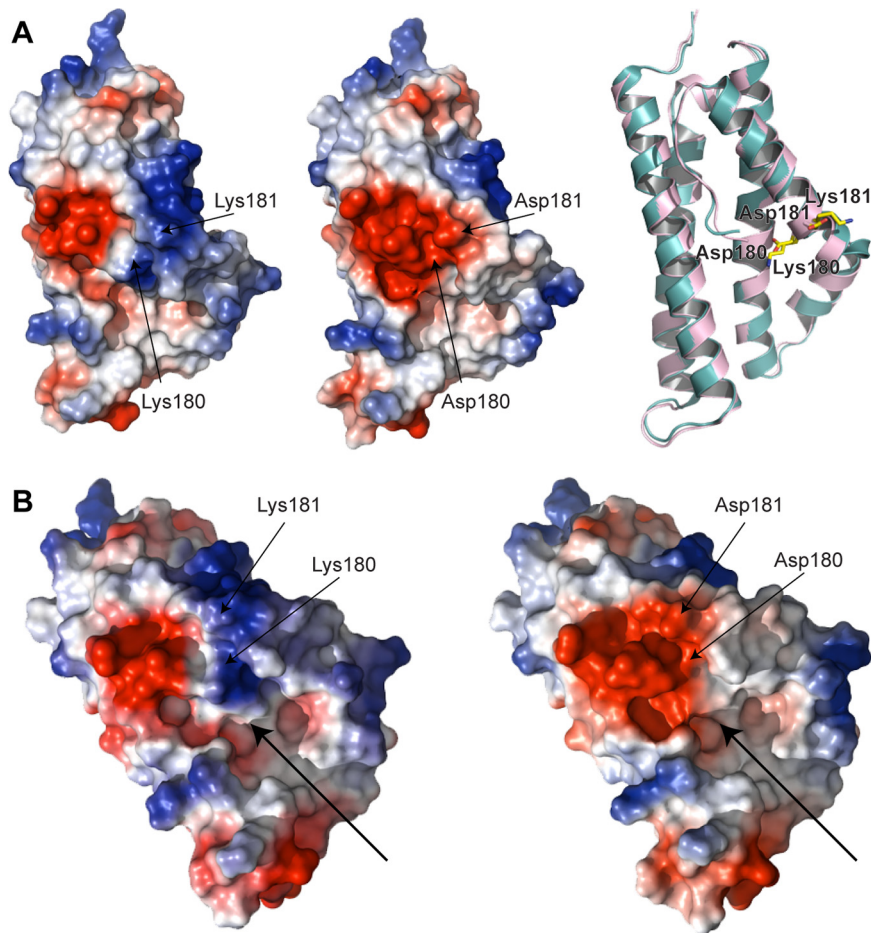


FIG 4 Structural comparison of LntA^{WT} and LntA^{K180D/K181D}. (A) Comparison of charged patches on the surfaces of LntA^{WT} (left) and LntA^{K180D/K181D} (middle). On the right, a ribbon overlay shows LntA^{WT} in light teal and LntA^{K180D/K181D} in light pink. The mutated residues are indicated as sticks. (B) Arrows indicate the direction of an elongated groove in the structures, which ends with the basic patch affected by the mutations.

uniformly distributed throughout the nucleoplasm and enriched neither at the Xi (Fig. 5) nor in small BAHD1 foci (Fig. S3B). The LntA^{K180R/K181R-V5} variant, which efficiently binds BAHD1 (Fig. 3B), still localized to BAHD1 foci and to the Xi.

To address the role of the cPRR in BAHD1, we also cotransfected LntA^{WT-V5} with a BAHD1^{ΔcPRR-YFP} deletion mutant lacking residues 239 to 361. Although this construct was able to form heterochromatin foci and was enriched at the Xi, its colocalization with LntA was impaired. We conclude that vicinity between LntA and BAHD1 in the nuclei of human cells is directly dependent on the K180/K181 motif in LntA and requires the integrity of the cPRR of BAHD1.

The K180/K181 dilysine motif is critical for LntA function. LntA stimulates IFN responses during bacterial infection of epithelial cells (10). This effect likely requires a cosignal triggered by the infection, since the direct expression of *lntA* in LoVo human colon adenocarcinoma cells did not affect the expression of representative ISGs (Fig. S4A). In cells infected with LntA-producing *Listeria*, the binding of BAHD1 to the promoter of ISGs decreases, while their expression increases (10), but whether this effect is a consequence of a direct interaction between LntA and BAHD1 is unknown. To address this issue, we examined the effect of the K180D and K181D mutations on LntA-induced IFN responses

during infection. We generated *L. monocytogenes* strains expressing *lntA*^{K180D/K181D} or *lntA*^{K180R/K181R} in fusion with a V5 tag as described previously for *lntA*^{WT} (10). The LntA^{K180D/K181D-V5} precursor was as efficiently produced and secreted into the culture medium after cleavage of the signal peptide as the wild-type form (Fig. S4B).

LoVo epithelial cells were infected for 18 h with these *lntA*-expressing strains or with a *lntA* deletion mutant carrying the empty vector (referred to as *lntA*^Δ), used as a control. There was no significant difference in the numbers of intracellular bacteria between strains (data not shown). Infection with *lntA*-expressing or -deficient bacteria triggered similar 30-fold inductions of the *IL8* proinflammatory cytokine gene (Fig. 6, left) over levels in noninfected cells. In contrast, while infection with *L. monocytogenes* *lntA*^Δ mildly stimulated expression of ISGs (e.g., *IFI6* and *IFITM1*), this effect was considerably enhanced in cells infected with *L. monocytogenes* *lntA*^{WT}, in agreement with our previous findings (10).

To examine the ability of LntA mutants to stimulate IFN responses, we monitored LntA-specific effects by normalizing data to the effect of *L. monocytogenes* *lntA*^Δ (Fig. 6, right). Remarkably, in contrast to *L. monocytogenes* *lntA*^{WT}, *L. monocytogenes* *lntA*^{K180D/K181D} failed to stimulate a number of ISGs (*CCL5*,

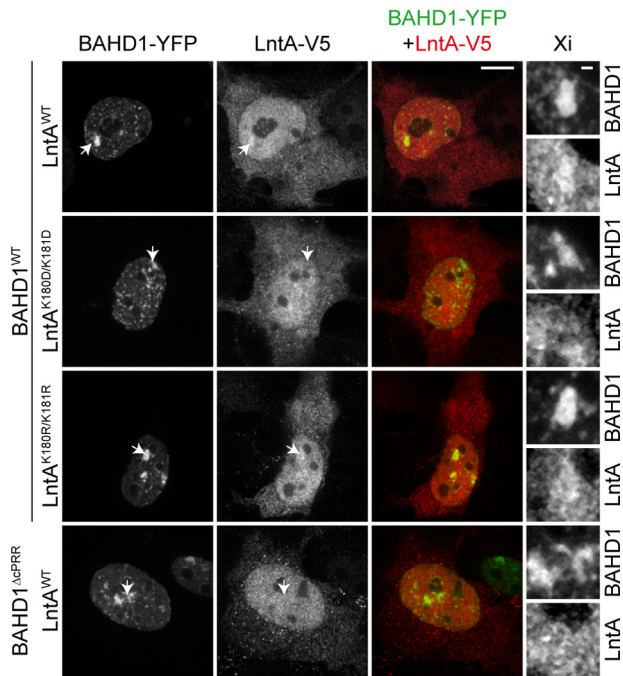


FIG 5 The K180/K181 dilysine motif in LntA and the proline-rich region in BAHD1 are required for the colocalization of the two proteins in human cells. 293FT cells were cotransfected for 48 h with WT or mutant versions of pcDNA3-LntA-V5 and pEYFP-N1-BAHD1. For *lntA*-V5, alleles resulted in WT, K180D/K181D, or K180R/K181R proteins. For *BAHD1*-YFP, alleles resulted in WT or Δ*PRR* (i.e., missing residues 239 to 361) proteins. LntA-V5 and BAHD1-YFP were detected by immunofluorescence confocal microscopy. Arrows indicate the position of an Xi. A magnification of these regions with enhanced contrasts is shown on the right. Bars, 10 μm for the cell view and 1 μm for magnified Xi regions.

IFI44L, *IFI6*, *IFIT1*, *IFIT2*, *IFIT3*, *IFITM1*, *ISG15*, and *MX1*) and interferon genes (*IFNB1* and *IL29*, which are themselves ISGs). Stimulation was reduced by 84.4% ± 13.9% compared to LntA^{WT}'s effect. This loss of function was reproducible in the JEG-3 placental epithelial cell line (stimulation was reduced by 92.4% ± 25.1% compared to LntA^{WT}'s effect) (Fig. S4C). In con-

trast, two LntA mutants whose binding to BAHD1 was not altered, *L. monocytogenes* *lntA*^{E91R} and *L. monocytogenes* *lntA*^{K180R/K181R}, behaved like *L. monocytogenes* *lntA*^{WT} in inducing the expression of ISGs (Fig. 6, right). Together, these results indicate that the K180/K181 dilysine motif in H5 and thus the direct interaction between LntA and BAHD1 are critical for LntA-mediated upregulation of ISGs during infection by *L. monocytogenes*.

LntA is highly conserved in all *L. monocytogenes* lineages. Since residues K180 and K181 in LntA play a key role in the interaction with BAHD1 and in an LntA-mediated stimulation of interferon responses, we wondered whether these residues were conserved in LntA from *L. monocytogenes* strains other than the reference strain EGD-e. To this aim, we sequenced the *lntA* open reading frame (ORF) from 188 strains representative of different lineages, serotypes, and origins. Strikingly, the *lntA* gene was present in all sequenced strains, without any deletion, and the amino acid sequence showed high conservation (Fig. S5A). We identified 19 sequence variants of the protein, most of which differed by only 1 residue from their nearest neighbor. The highest occurrence of variability was found in the N-terminal region, encompassing the first 23 amino acids of the secreted protein (residues 34 to 56). This region could not be traced in the crystallographic structure, suggesting a higher flexibility. N-terminal variation was particularly obvious in a subset of 1/2b strains of the ST5/59 sequence type defined by multilocus sequence typing (MLST) (19). Among other residues exposed on the LntA surface, the key K180/K181 dilysine motif was conserved in all LntA sequences.

The strong conservation of LntA in *L. monocytogenes* suggests a selective pressure to maintain the gene and the sequence of the basic patch required for its function through interaction with BAHD1. In addition, this gene is absent in nonpathogenic *Listeria* species, consistent with its role in pathogenesis. There is, however, one exception, since *lntA* has a homolog in *Listeria marthii*, a close nonpathogenic relative of *L. monocytogenes*. LntA from *L. marthii* FSL S4-120 (20) shows 76.2% sequence identity with LntA from *L. monocytogenes* strain EGD-e; the critical K180 and K181 residues are conserved, but three residues in the neighboring region are different (Fig. S5A). The N-terminal region of the mature *L. marthii* LntA protein also diverges from *L. monocytogenes* LntA.

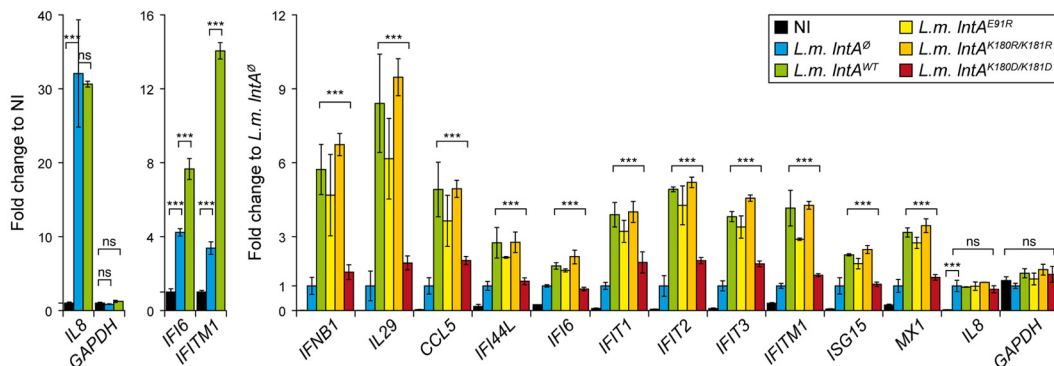


FIG 6 Stimulation of ISG expression by LntA during infection is impaired by mutation of the K180/K181 dilysine motif. Innate immune gene expression was quantified by RT-qPCR in noninfected LoVo cells (NI) or cells infected for 18 h with *L. monocytogenes* *lntA*^Δ, *lntA*^{WT}, *lntA*^{K180R/K181R}, or *lntA*^{K180D/K181D} (left). Induction of the expression of interleukin 8 (IL-8), *IFI6*, and *IFITM1* by *L. monocytogenes* *lntA*^Δ and *L. monocytogenes* *lntA*^{WT}, compared to uninfected cells (right). LntA-dependent induction of ISGs, monitored by normalization to cells infected with *L. monocytogenes* *lntA*^Δ. Error bars indicate standard deviations. The reference gene for normalization was *YWHAZ*; *GAPDH* was a control invariant gene. Statistical analysis was performed using analysis of variance (ANOVA) followed by the Tukey-Kramer posttest. ns, nonsignificant; ***, *P* < 0.001.

In addition, the promoter regions of the *lntA* genes differ between the two species (Fig. S5B). Of note, the binding site for PrfA, a major transcriptional regulator of virulence genes in *L. monocytogenes*, is degenerated in the *L. marthii* *lntA* promoter. This is consistent with *prfA* being absent in *L. marthii*. Additionally, a 70-nucleotide sequence upstream of the ribosome binding site brings a putative recognition site for σ^B and therefore potentially an alternative regulation mechanism. The virulence-specific regulation of the expression of *lntA* thus does not seem to be conserved in this environmental *Listeria* species.

DISCUSSION

The secreted virulence factor LntA from *Listeria monocytogenes* belongs to the growing number of bacterial effectors called nucleomodulins, which exert their function by entering the host cell nucleus and hijacking nuclear processes (14). So far, LntA constitutes a unique example of a bacterial protein capable of interacting with a chromatin repressor, BAHD1, thus causing its release from its target ISGs and upregulating interferon responses (10, 12). In this study, we explored in molecular detail the mechanisms of the LntA-BAHD1 interplay. We identified a conserved basic motif on the surface of LntA and a central region in BAHD1 as key elements for the interaction between the two proteins.

To better understand the mechanisms of BAHD1 inhibition by LntA, these interface elements need to be envisaged in the context of the whole proteins. The relative contribution of the distinct BAHD1 domains to its function has not been thoroughly explored. The most characteristic region in BAHD1 is the C-terminal BAH domain, present in a number of chromatin-bound proteins, components of chromatin-remodeling complexes, or origin recognition complexes (reviewed in reference 16). Interestingly, BAH domain proteins (RERE, MTA1, BAF180/hPB1, ASH1L/KMT2H, TNRC18) often also contain low-complexity sequences, including proline-rich regions, which provide additional possibilities for intermolecular interactions (reviewed in reference 21). Likewise, by bridging distinct functional modules together, BAHD1 is thought to constitute a scaffold for the assembly and spreading of a heterochromatic complex at target loci (15).

The BAHD1 region that interacts with LntA was mapped in the central part of the protein (residues 187 to 428) by 2-hybrid screening (10) and encompasses a central proline-rich region (residues 239 to 361). Here, we document that only the fragment from residues 187 to 428 can stably bind LntA *in vitro* and that the cPRR alone is not sufficient to bind its partner molecule. Reciprocally, LntA cannot colocalize with a BAHD1 deletion mutant devoid of the cPRR, even though the overall features of this construct, such as its ability to form heterochromatin foci and localize to the Xi, are unaffected. Both the BAHD1 cPRR and its flanking regions are therefore important for a stable interaction with LntA. Thus, in addition to providing a better understanding of the LntA-BAHD1 interplay, this work pinpoints a potential role of the BAHD1 proline-rich region as a docking module involved in the regulation of the activity of its associated complex.

The secreted form of LntA can be subdivided into two domains; the trunk of the protein is formed by a bundle of helices, H1 to H3, while H4 and H5 protrude from one side of the protein. The positioning of the elbow relative to the trunk creates an elongated groove on LntA's surface, lined by charged patches. We identified the K180/K181 dilysine motif on the surface of helix H5

as essential for BAHD1 recognition and, as a consequence, LntA function. The LntA^{K180D/K181D} double mutant is unable to bind BAHD1 *in vitro* or to colocalize within BAHD1-induced chromatin foci in cells. This mutant also shows a reduced ability to stimulate ISGs during *Listeria* infection of epithelial cells. The crystal structure of LntA^{K180D/K181D}, with a fold highly similar to that of the wild-type molecule, reveals that the double mutation significantly modifies the pattern of charges decorating the bottom end of the elongated groove, which, based on its size and shape, may potentially accommodate a peptide sequence from BAHD1. Apart from the elbow region of LntA involved in BAHD1 recognition, the H1-to-H3 trunk remains potentially free for interacting with other components. Further exploration of the binding partners and function of this part of LntA might, in the future, provide a basis for LntA specificity to ISGs from among the variety of BAHD1 target genes.

The manipulation of human gene expression is of critical importance for the invasion, proliferation, and survival of bacteria during infection and must be carefully timed and tuned. Among the virulence factors that *Listeria* employs to control the immune response of its host, LntA stimulates the interferon pathway through its interaction with BAHD1 at a step of infection which remains unknown. Although the constitutive expression of *lntA* by bacteria is detrimental to the infectious process (10), we report here that the *lntA* gene is conserved in all *L. monocytogenes* lineages, showing no deletion or nonsense mutation and very little variation in the amino acid sequence of the protein product. In particular, the critical K180 and K181 residues are conserved. In contrast, a number of other *Listeria* virulence factors are not as well conserved (22). For instance, the gene encoding internalin, a critical factor for cell invasion, displays premature stop codons in several *L. monocytogenes* isolates, leading to a truncated secreted protein (19, 23, 24). In comparison, *lntA* robustness suggests the existence of high selective pressure for the conservation of LntA's functionality. Meanwhile, the tight regulation of *lntA* expression (10) pinpoints a strong requirement for its limitation to an optimal spatiotemporal frame during the infectious process.

The *lntA* gene is absent from all other *Listeria* species, except in the closely related nonpathogenic species *L. marthii*, as highlighted in a response to our previous work (25). However, in this environmental species, the LntA amino acid sequence displays mutations that might affect its function, and the promoter of the *lntA* gene is mutated in the binding site for the major regulator of virulence genes, PrfA. The evolution of the *lntA* promoter toward non-virulence-related regulations might point to a divergent role for this form of LntA.

LntA seems to be unique to *Listeria*, as no similar proteins can be found by BLAST search. However, one cannot exclude the possibility that structural or functional homologs might be found in future studies. The interaction region of LntA and BAHD1 constitutes a potential target for development of molecules that may control interferon responses or the expression of other BAHD1 target genes. Although the structure of full-length BAHD1 is still unsolved and such studies would be challenging due to the large predicted unstructured regions, in-depth structural and functional characterization will be required for the detailed comprehension of the mechanism of BAHD1 repression of its target genes.

MATERIALS AND METHODS

Bacterial strains, human cell lines, plasmids, and antibodies. Strains and plasmids used in this work are recapitulated in Tables S2, S3, and S4, respectively. Details about plasmid constructs, human cell lines, and antibodies are provided in Text S1 in the supplemental material.

Gel filtration. LntA was purified from *E. coli* BL21(DE3) as described previously (10). GST-BAHD1 constructs were expressed in *E. coli* BL21-CodonPlus(DE3)-RIL (Stratagene); cultures were induced with 1 mM IPTG (isopropyl- β -D-thiogalactopyranoside) when the optical density at 600 nm (OD₆₀₀) attained a value of 0.5 to 0.8. Induction was performed at 30°C for 3 h for GST-BAHD1^{187–428} or at 20°C overnight for GST-BAHD1^{239–361}. Cells were lysed and purified as described in reference 10 on 5-ml GST-Trap columns. LntA (without its tag) and the two GST-BAHD1 proteins were injected separately or incubated at a 1:1 molar ratio for 3 h at 4°C prior to injection on a Superdex 200 HR 10/30 column equilibrated in 25 mM HEPES (pH 7.5), 0.1 M NaCl, and 5% glycerol. Eluted fractions were analyzed by SDS-PAGE and stained with Coomassie blue G.

Coexpression in *E. coli* and pulldown experiments. *E. coli* BL21(DE3) cells harboring both pGEX-BAHD1 and pACYDuet-LntA plasmids were grown in 250 ml Luria-Bertani (LB) medium at 37°C up to an OD₆₀₀ value of 0.5 to 0.8 and induced with 1 mM IPTG for 3 h. Bacterial pellets were lysed by sonication in 25 mM Tris-HCl (pH 8.5), 0.2 M NaCl, 10% glycerol, 1 mM EDTA (buffer A) in the presence of DNase I and protease inhibitor cocktail. Extracts were clarified at 30,000 × g and loaded onto 1-ml His-Trap or GST-Trap columns (GE Healthcare), pre-equilibrated in buffer A. The complexes were eluted with the same buffer containing 20 mM reduced glutathione (GST-Trap) or 500 mM imidazole (His-Trap). All fractions were analyzed by SDS-PAGE and immunoblotting. Pulldown experiments were repeated four times on the GST-Trap and twice on the His-Trap columns.

Crystallization, data collection, structure solution. For the crystallization of Se-methionine LntA^{K180D/K181D}, the protein was expressed as a GST fusion in M9 minimal medium containing 200 mg/liter thiamine. When cultures had attained an OD₆₀₀ value of 0.5, 60 mg of Se-Met, 100 mg of L-Lys, L-Phe, and L-Thr, and 50 mg of L-Iso, L-Leu, and L-Val were added per liter of culture. After 30 min of growth, expression was induced by the addition of 1 mM IPTG. The protein was then purified as described previously for wild-type LntA (10) except that the last step of purification was on a Superdex 200 HR 10/30 column in 25 mM KPi (pH 7.0), 0.2 M NaCl, 1 mM dithiothreitol (DTT). Full labeling by selenium atoms was confirmed by mass spectrometry.

Crystallization tests were performed at 4°C on the HTX-PSB platform in Grenoble, France. Crystals were grown with a protein concentration of 5 mg/ml at 20°C using the hanging-drop technique in 0.1 M citrate (pH 5.0), 1 M LiCl₂, and 21% polyethylene glycol 3350. Crystals were cryoprotected in 25% glycerol prior to data collection.

A single data set was collected on beamline BM14 (ESRF, Grenoble, France), and MR phasing was performed by Phaser (25) using the structure of wild-type LntA (PDB accession number 2XL4) as a search model. Further model improvement was done by manual model building using Coot (27) and remlac (28) by an amplitude-based twin-refinement protocol. Final data collection, structure solution, and refinement statistics are shown in Table S1.

GST pulldown experiments on solubilized chromatin extracts from transfected cells. GST-InlC or -LntA fusion proteins were produced from BL21(DE3) transformed with pGEX-derived plasmids. Fifty-milliliter samples of cultures at an OD₆₀₀ of 0.6 were induced with 0.3 mM IPTG and grown for 3 h at 30°C. Bacterial pellets were lysed for 30 min at 4°C in lysis buffer (50 mM Tris-HCl, pH 7.6, 300 mM NaCl, 1% Triton X-100, 5% glycerol, 50 μ g/ml lysozyme, 1 mM MgCl₂, 1 U/ml Benzonase [Novagen]). Extracts were clarified at 20,000 × g at 4°C for 10 min. Bacterial extracts were preincubated with glutathione-Sepharose 4B resin (GE Healthcare Life Sciences) for 1.5 h at 4°C on a rotating wheel (10 rpm). Beads were washed 5× in 1 ml wash buffer (30 mM Tris, pH 8, 150 mM

NaCl, 10% glycerol, 0.5 mM EDTA, 0.1% IGEPAL) before incubation with chromatin extracts. All buffers were supplemented with EDTA-free Complete protease inhibitor cocktail (Roche).

293FT cells were transfected for 48 h with pcDNA3.1/V5-His-TOPO-*mCFP* or pcDNA3.1/V5-His-TOPO-*BAHD1*, with Lipofectamine LTX (Life Technologies), used as specified by the manufacturer. Solubilized chromatin extracts were prepared as described for protein complex immunoprecipitation (29). Briefly, transfected cells (5 × 10⁶ per GST pull-down assay) were fractionated into cytoplasmic, nuclear soluble, and chromatin fractions. The chromatin fraction was solubilized by digestion with micrococcal nuclease (Sigma), followed by sonication in a Bioruptor (Diagenode). Extracts were clarified by centrifugation at 20,000 × g and 4°C for 10 min.

Pulldown assays were performed by mixing chromatin extracts containing the V5-tagged preys with glutathione-Sepharose beads prebound to GST-tagged baits. The input composition was 150 mM NaCl, 30 mM Tris-HCl (pH 8.0), 27 mM sucrose, 9% glycerol, 0.7 mM EDTA, 0.05 mM spermidine, 1 mM DTT, 0.01% IGEPAL. After cells were bound for 4 h at 4°C and washed, elution was performed by direct addition of 50 μ l of SB2X. Input and eluted samples were analyzed by SDS-PAGE and immunoblotting against the V5 tag and by colloidal Coomassie blue staining. Figure 3B is representative of 2 distinct experiments performed with independently produced protein batches.

Immunofluorescence on transfected cells, confocal microscopy, image processing, and analysis. 293FT cells were seeded 24 h before transfection in 24-well plates containing 12-mm-diameter coverslips pre-coated with poly-L-lysine. Transfections were performed using Lipofectamine LTX (Invitrogen) according to the manufacturer's specifications. Forty-eight hours after transfection, cells were fixed for 20 min with 4% paraformaldehyde in phosphate-buffered saline (PBS) and then permeabilized for 5 min at room temperature with 0.5% Triton X-100 in CSK buffer [100 mM NaCl, 300 mM sucrose, 3 mM MgCl₂, 10 mM PIPES (pH 6.8), 1.2 mM 4-(2-aminoethyl)benzenesulfonyl fluoride hydrochloride (AEBSF)] and for 5 min in CSK buffer containing 2% bovine serum albumin (BSA; Sigma). Incubation with anti-V5 primary antibody in CSK buffer, 1% BSA was performed for 1 h and with the Cy3-conjugated secondary antibody and DAPI (4',6-diamidino-2-phenylindole; 0.1 μ g/ml) for 30 min. Cover glasses were finally mounted on microscope slides with Fluoromount mounting medium (Interchim).

Preparations were observed with an Axio Observer.Z1 microscope (Zeiss) coupled to a spinning-disk confocal device (model CSU-XI; Yokogawa), connected to a cooled electron microscopy charge-coupled-device (EM-CCD) camera (Evolve; Photometrics). Images were acquired with Apochromat 100× (numerical aperture, 1.4) objective lenses in 2-mm-high, 200- μ m-step Z-stacks with the MetaMorph software, version 7.7.9.0 (Molecular Devices). Acquisition parameters were similar for all samples. For snapshot display, maximum intensity signals from 4 successive stacks (i.e., 0.6- μ m slices) were integrated with ImageJ. Each picture is representative of the transfected cell population observed in two independent experiments.

Cellular infections. Cells were seeded in 24-well plates to achieve a density at the time of infection of 2.5 × 10⁵ cells/well for LoVo cells and 1 × 10⁵ cells/well for JEG-3 cells. *Listeria* strains were grown in brain heart infusion (BHI) medium to an OD₆₀₀ of 3, washed in PBS, and diluted in culture medium without serum to achieve a multiplicity of infection (MOI) of 10. Bacterial inoculums were added to cell plates and centrifuged for 1 min at 200 × g to synchronize entry. After 1 h, cells were washed twice and the remaining noninvasive bacteria were killed by adding culture medium containing 20 μ g/ml gentamicin. The quantification of intracellular bacteria was done at 18 h postinfection (p.i.). Infected cells were washed in PBS and then disrupted in sterile water for 10 min at 4°C. Triplicates of serial dilutions were plated on BHI agar; the numbers of CFU were determined on the next day.

RNA extraction and reverse transcription-quantitative PCR (RT-qPCR). In infected LoVo or JEG-3 cells, RNA was extracted at, respec-

tively, 18 or 20 h p.i. with an RNeasy minikit (Qiagen) as recommended by the manufacturer, using 1 column per well of a 24-well plate and biological duplicates for each condition. Genomic DNA was removed by treatment with a Turbo DNA-free kit (Ambion). cDNAs were generated from 1 to 2 μ g total RNA using the RT² HT first-strand kit (Qiagen/SABiosciences).

qPCR was performed on a CFX384 instrument (Bio-Rad) using Kapa SYBR Fast universal master mix (Kapa Biosystems) as specified by the supplier. Each reaction was performed in triplicate. RT-qPCR primers for *YWHAZ*, *IFI44L*, *IFITM1*, and *IL6* were pre-designed, validated RT² qPCR primer pairs from Qiagen/SABiosciences. Other primer pairs were selected from the literature, from primer databases (RTPrimerDB, <http://medgen.ugent.be/rtpriprimerdb/>), or qPrimerDepot, <http://primerdepot.nci.nih.gov/>) and validated for efficiency. Data were analyzed by the $\Delta\Delta C_T$ method. Target gene expression data were normalized to the relative expression of the *YWHAZ* reference gene. The displayed results are representative of three independent experiments in LoVo cells and two experiments in JEG-3 cells.

Protein structure accession number. The structural data from this publication have been submitted to the Protein Data Bank (<http://www.rcsb.org/pdb/>) and assigned the identifier 4CIH.

SUPPLEMENTAL MATERIAL

Supplemental material for this article may be found at <http://mbio.asm.org/lookup/suppl/doi:10.1128/mBio.00775-13/-/DCSupplemental>.

Figure S1, TIF file, 12.4 MB.
Figure S2, TIF file, 3.1 MB.
Figure S3, TIF file, 15 MB.
Figure S4, TIF file, 7.3 MB.
Figure S5, TIF file, 17.5 MB.
Table S1, DOCX file, 0.1 MB.
Table S2, DOCX file, 0.1 MB.
Table S3, DOCX file, 0.1 MB.
Table S4, DOCX file, 0.2 MB.
Text S1, DOCX file, 0.1 MB.

ACKNOWLEDGMENTS

We are grateful to Morwena Leguillou and Jean Feunteun for providing the BAHD1 ^{Δ cPRR} construct, Alexandre Leclercq for help with the *L. monocytogenes* strain database, Goran Lakisic for help with protein production, Marjolaine Noirclercq-Savoie for help with testing the solubility of LntA variants, Adrien Favier for performing 1D-NMR experiments on LntA mutants, Luca Signor for performing spectrometry measurements on LntA, J. Marquez and the HTX Lab team for access to and help with high-throughput crystallization, the ESRF for access to beamlines, Babu Manjasetty, Hassan Berlhali (BM14, ESRF), and Carlos Contreras-Martel (IBS) for help with data processing and structure solution, and Andrey Grishin for critical reading of the manuscript. This work used the platforms of the Grenoble Instruct Centre (ISBG; UMS 3518 CNRS-CEA-UJF-EMBL) within the Grenoble Partnership for Structural Biology (PSB).

This work received funding from INRA, CNRS, and the Pasteur Institute, as well as French National Research Agency grants EPILIS (ANR-11-BSV3 003-01), FRISBI (ANR-10-INSB-05-02), and GRAL (ANR-10-LABX-49-01), and from European Research Council (ERC) Advanced grant 233348. P. Cossart is a Senior International Research Scholar of the Howard Hughes Medical Institute.

REFERENCES

- Allerberger F, Wagner M. 2010. Listeriosis: a resurgent foodborne infection. *Clin. Microbiol. Infect.* 16:16–23. <http://dx.doi.org/10.1111/j.1469-0691.2009.03109.x>.
- Stavru F, Archambaud C, Cossart P. 2011. Cell biology and immunology of *Listeria monocytogenes* infections: novel insights. *Immunol. Rev.* 240:160–184. <http://dx.doi.org/10.1111/j.1600-065X.2010.00993.x>.
- Zenewicz LA, Shen H. 2007. Innate and adaptive immune responses to *Listeria monocytogenes*: a short overview. *Microbes Infect.* 9:1208–1215. <http://dx.doi.org/10.1016/j.micinf.2007.05.008>.
- Camejo A, Carvalho F, Reis O, Leitão E, Sousa S, Cabanes D. 2011. The arsenal of virulence factors deployed by *Listeria monocytogenes* to promote its cell infection cycle. *Virulence* 2:379–394. <http://dx.doi.org/10.4161/viru.2.5.17703>.
- Cossart P. 2011. Illuminating the landscape of host-pathogen interactions with the bacterium *Listeria monocytogenes*. *Proc. Natl. Acad. Sci. U. S. A.* 108:19484–19491. <http://dx.doi.org/10.1073/pnas.1112371108>.
- Freitag NE, Port GC, Miner MD. 2009. *Listeria monocytogenes*—from saprophyte to intracellular pathogen. *Nat. Rev. Microbiol.* 7:623–628. <http://dx.doi.org/10.1038/nrmicro2171>.
- Bierne H, Cossart P. 2002. InlB, a surface protein of *Listeria monocytogenes* that behaves as an invasin and a growth factor. *J. Cell Sci.* 115:3357–3367.
- Gouin E, Adib-Conquy M, Balestrino D, Nahori MA, Villiers V, Coland F, Dramsi S, Dussurget O, Cossart P. 2010. The *Listeria monocytogenes* InlC protein interferes with innate immune responses by targeting the I κ B kinase subunit IKK α . *Proc. Natl. Acad. Sci. U. S. A.* 107:17333–17338. <http://dx.doi.org/10.1073/pnas.1007765107>.
- Hamon MA, Batsché E, Régnauld B, Tham TN, Seveau S, Muchardt C, Cossart P. 2007. Histone modifications induced by a family of bacterial toxins. *Proc. Natl. Acad. Sci. U. S. A.* 104:13467–13472. <http://dx.doi.org/10.1073/pnas.0702729104>.
- Lebreton A, Lakisic G, Job V, Fritsch L, Tham TN, Camejo A, Mattei PJ, Régnauld B, Nahori MA, Cabanes D, Gautreau A, Ait-Si-Ali S, Dessen A, Cossart P, Bierne H. 2011. A bacterial protein targets the BAHD1 chromatin complex to stimulate type III interferon response. *Science* 331:1319–1321. <http://dx.doi.org/10.1126/science.1200120>.
- Hamon MA, Cossart P. 2011. K⁺ efflux is required for histone H3 dephosphorylation by *Listeria monocytogenes* listeriolysin O and other pore-forming toxins. *Infect. Immun.* 79:2839–2846. <http://dx.doi.org/10.1128/IAI.01243-10>.
- Lebreton A, Cossart P, Bierne H. 2012. Bacteria tune interferon responses by playing with chromatin. *Virulence* 3:87–91. <http://dx.doi.org/10.4161/viru.3.1.18531>.
- Bierne H, Hamon M, Cossart P. 2012. Epigenetics and bacterial infections. *Cold Spring Harb Perspect. Med* 2:a010272. <http://dx.doi.org/10.1101/cshperspect.a010272>.
- Bierne H, Cossart P. 2012. When bacteria target the nucleus: the emerging family of nucleomodulins. *Cell. Microbiol.* 14:622–633. <http://dx.doi.org/10.1111/j.1462-5822.2012.01758.x>.
- Bierne H, Tham TN, Batsche E, Dumay A, Leguillou M, Kernéis-Golsteyn S, Régnauld B, Seeler JS, Muchardt C, Feunteun J, Cossart P. 2009. Human BAHD1 promotes heterochromatic gene silencing. *Proc. Natl. Acad. Sci. U. S. A.* 106:13826–13831. <http://dx.doi.org/10.1073/pnas.0901259106>.
- Yang N, Xu RM. 2013. Structure and function of the BAH domain in chromatin biology. *Crit. Rev. Biochem. Mol. Biol.* 48:211–221. <http://dx.doi.org/10.3109/10409238.2012.742035>.
- Barandun J, Delley CL, Weber-Ban E. 2012. The pupylation pathway and its role in mycobacteria. *BMC Biol.* 10:95. <http://dx.doi.org/10.1186/1741-7007-10-95>.
- Jones JD, O'Connor CD. 2011. Protein acetylation in prokaryotes. *Proteomics* 11:3012–3022. <http://dx.doi.org/10.1002/pmic.201000812>.
- Ragon M, Wirth T, Hollandt F, Lavenir R, Lecuit M, Le Monnier A, Brisse S. 2008. A new perspective on *Listeria monocytogenes* evolution. *PLoS Pathog.* 4:e1000146. <http://dx.doi.org/10.1371/journal.ppat.1000146>.
- den Bakker HC, Cummings CA, Ferreira V, Vatta P, Orsi RH, Degoricija L, Barker M, Petrauskene O, Furtado MR, Wiedmann M. 2010. Comparative genomics of the bacterial genus *Listeria*: genome evolution is characterized by limited gene acquisition and limited gene loss. *BMC Genomics* 11:688. <http://dx.doi.org/10.1186/1471-2164-11-688>.
- Kay BK, Williamson MP, Sudol M. 2000. The importance of being proline: the interaction of proline-rich motifs in signaling proteins with their cognate domains. *FASEB J.* 14:231–241.
- Kuenne C, Billion A, Mraheil MA, Strittmatter A, Daniel R, Goesmann A, Barbuddhe S, Hain T, Chakraborty T. 2013. Reassessment of the *Listeria monocytogenes* pan-genome reveals dynamic integration hotspots and mobile genetic elements as major components of the accessory ge-

- nome. BMC Genomics 14:47. <http://dx.doi.org/10.1186/1471-2164-14-47>.
23. Jonquières R, Bierne H, Mengaud J, Cossart P. 1998. The *inlA* gene of *Listeria monocytogenes* LO28 harbors a nonsense mutation resulting in release of internalin. Infect. Immun. 66:3420–3422.
24. Jacquet C, Doumith M, Gordon JI, Martin PM, Cossart P, Lecuit M. 2004. A molecular marker for evaluating the pathogenic potential of food-borne *Listeria monocytogenes*. J. Infect. Dis. 189:2094–2100. <http://dx.doi.org/10.1086/420853>.
25. den Bakker HC, Wiedmann M. 16 May 2011. New *Listeria* virulence gene also found in a non-pathogenic *Listeria* species. Science. http://www.sciencemag.org/content/331/6022/1319.abstract/reply#sci_el_14407.
26. McCoy AJ, Grosse-Kunstleve RW, Adams PD, Winn MD, Storoni LC, Read RJ. 2007. Phaser crystallographic software. J. Appl. Crystallogr. 40: 658–674. <http://dx.doi.org/10.1107/S0021889807021206>.
27. Emsley P, Cowtan K. 2004. Coot: model-building tools for molecular graphics. Acta Crystallogr. D Biol. Crystallogr. 60:2126–2132. <http://dx.doi.org/10.1107/S0907444904019158>.
28. Murshudov GN, Vagin AA, Dodson EJ. 1997. Refinement of macromolecular structures by the maximum-likelihood method. Acta Crystallogr. D Biol. Crystallogr. 53:240–255. <http://dx.doi.org/10.1107/S0907444996012255>.
29. Fritsch L, Robin P, Mathieu JR, Souidi M, Hinaux H, Rougeulle C, Harel-Bellan A, Ameyar-Zazoua M, Ait-Si-Ali S. 2010. A subset of the histone H3 lysine 9 methyltransferases Suv39h1, G9a, GLP, and SETDB1 participate in a multimeric complex. Mol. Cell 37:46–56. <http://dx.doi.org/10.1016/j.molcel.2009.12.017>.